Acta Crystallographica Section B
Structural Science
ISSN 0108-7681

Change in electronic structure in a six-coordinate copper(II) complex accompanied by an anion order/disorder transition

Colin A. Kilner and Malcolm A. Halcrow*

Department of Chemistry, University of Leeds, Leeds LS2 9IT, England

Correspondence e-mail: m.a.halcrow@leeds.ac.uk

Received 16 October 2009
Accepted 29 January 2010

A variable-temperature crystallographic study of $[Cu(L^{OH})_2][ClO_4]_2{\cdot}2(CH_3)_2CO$ [L^{OH} = 2,6-bis(hydroxyiminomethyl)pyridine] between 30 and 300 K is presented. The complex exhibits an unusual electronic structure at room temperature with a $\{d_{z^2}\}^1$ ground state, corresponding to an axially compressed ligand coordination geometry about the copper ion. This reflects a suppression of the pseudo-Jahn–Teller distortion that is normally shown by copper(II) compounds with this ligand geometry [Halcrow *et al.* (2004). *New J. Chem.* **28**, 228–233]. On cooling the compound undergoes an abrupt structural change at 157 ± 3 K, that does not involve a change in the space group ($P\bar{1}$), but causes significant changes to *c* and the unit-cell angles. This reflects a conformational rearrangement of the complex dication, towards a more typical pseudo-Jahn–Teller elongated coordination geometry. This occurs concurrently with a crystallographic ordering of one of the two perchlorate anions, and a significant displacement of the two lattice acetone molecules. The transformation involves displacements of up to 0.5 Å in the non-H atoms of the structure at 30 K, compared with their positions at 300 K. The change in coordination geometry of the complex around 157 K is reflected in a small reduction in its magnetic moment near that temperature.

1. Introduction

The vast majority of six-coordinate copper(II) complexes adopt a (pseudo)-Jahn–Teller elongated structure in solution and the solid state, corresponding to a $\{d_{x^2-y^2}\}^1$ electronic ground state (Hitchman, 1994; Falvello, 1997; Murphy & Hathaway, 2003). This reflects a small energetic stabilization of the d_{z^2} orbital at the copper ion through $4s/3d_{z^2}$ mixing, which intrinsically favours the Jahn–Teller elongation over the alternative, an axially compressed molecular structure with a $\{d_{z^2}\}^1$ electronic configuration. Distinguishing these two situations crystallographically can be a challenge, because the unique axis of the Jahn–Teller distortion can be masked by static or dynamic disorder about the metal coordination sphere (Falvello, 1997). Similar disorder effects can also be seen in the EPR spectra of solid copper(II) compounds. Thus, several proposals of Jahn–Teller compressions in copper(II) complexes in the earlier literature have since been reassigned as disordered Jahn–Teller elongated structures following more detailed variable-temperature crystallography, EPR and/or EXAFS experiments (Halcrow, 2003). There are no confirmed Jahn–Teller compressed copper(II) molecular complexes, although a small number of inorganic copper(II) materials do possess that structure (Halcrow, 2003, and references therein; Mazej *et al.*, 2004).

Ten years ago, we first reported that the electronic structure of D_{2d}-symmetric copper(II) complexes of meridional tridentate imine ligands can be controlled, by steric or conformational effects (Solanki *et al.*, 1998, 2001; Bridgeman *et al.*, 1999; Holland *et al.*, 2000). Thus, for example, homoleptic copper(II) complexes of 2,6-bis(iminomethyl)pyridine derivatives (L^R, Fig. 1) can adopt two different electronic structures, depending on the identity of the '*R*' substituents (Holland *et al.*, 2000; Salaudeen *et al.*, 2008). Smaller substituents like methyl, cyclohexyl or a benzyl derivative give complexes with the usual pseudo-Jahn–Teller elongated structure by crystallography and/or EPR, which in this case corresponds to a lengthening of two of the distal Cu—N{aldimine} bonds (structure *A*, Fig. 1). However, larger *tert*-butyl '*R*' groups disfavour such a structure, because of steric interactions between the *tert*-butyl groups on one ligand and the pyridyl ring of the other. This enforces an alternative, axially compressed molecular structure onto the molecule, with a concomitant change in its electronic configuration to $\{d_{z^2}\}^1$ by EPR (*B* in Fig. 1). Structure *B* is not a Jahn–Teller compression, because the e_g *d*-orbitals are not degenerate in the idealized D_{2d} symmetry shown by these compounds. Rather, it corresponds to a suppression of the pseudo-Jahn–Teller elongation in structure *A*. A suppressed pseudo-Jahn–Teller effect of this type is also seen in the one-dimensional chain structure β-$[CuBr_2(NH_3)_2]$ (Obert & Bersuker, 1983) and a few structurally related copper-doped materials (van Ooijen *et al.*, 1977; Riley *et al.*, 1988). However, these are the only molecular copper(II) complexes to show this unusual effect.

During this work, we noted that the solid oxime and hydrazone derivatives of $[Cu(L^R)_2][ClO_4]_2$ [Fig. 1, *R* = OH (I) or NH_2 (II)] also adopt structure *B* at room temperature, which we attributed to the reduced basicity of their aldimino N donor atoms bearing electron-withdrawing heteroatom '*R*' substituents (Halcrow *et al.*, 2004). However, at 100 K their EPR and/or crystallographic behaviour more closely resembles that expected from structure *A*, implying that the compounds may exhibit an unprecedented thermally induced ground-state switching. The complexes also adopt structure *A* in solution as shown by EPR, implying that this unusual temperature-dependent behaviour is purely a solid-state phenomenon. We present here a full variable-temperature crystallographic and magnetic susceptibility study of the solvate $[Cu(L^{OH})_2][ClO_4]_2{\cdot}2(CH_3)_2CO$ [(I)·2$(CH_3)_2$CO], to elucidate the structural origin of this novel effect.

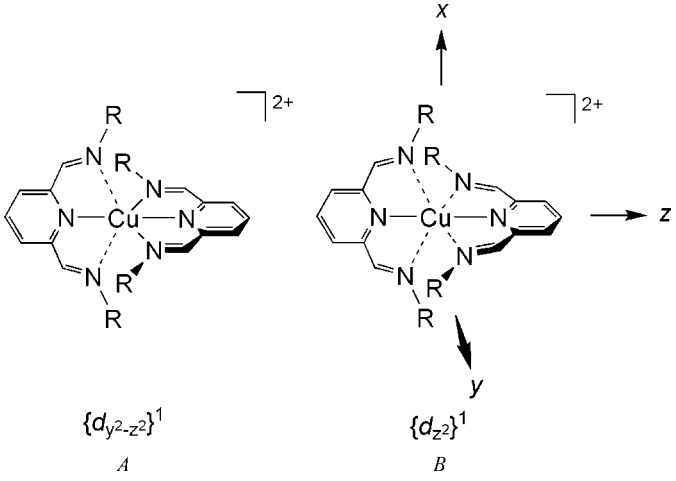

Figure 1
The two structures adopted by $[Cu(L^R)_2]^{2+}$ complexes, and their corresponding electronic ground-state configurations. Short and long Cu—N bonds are indicated by solid and dashed lines, respectively. The $\{d_{y^2-z^2}\}^1$ configuration for structure *A* is equivalent to the more familiar $\{d_{x^2-y^2}\}^1$. The $\{d_{y^2-z^2}\}^1$ nomenclature reflects the fact that the pseudo-Jahn–Teller elongation in structure *A* does not lie on the unique symmetry axis (*z*) of the molecule.

2. Experimental

2.1. Crystal growth

Compound (I) was prepared by a previously reported method (Halcrow *et al.*, 2004). Vapour diffusion of diethyl ether into a dilute acetone solution of (I) at room temperature afforded well formed green rectangular prisms of the solvate (I)·2$(CH_3)_2$CO. These crystals rapidly decompose upon exposure to air, yielding a solvent-free green powder. Found: C 28.6, H 2.35, N 14.3%; calcd. for $C_{14}H_{14}CuCl_2N_6O_{12}$: C 28.4, H 2.38, N 14.2%. The attempted crystallization of (I) from other organic solvents led to its decomposition to a brown oil over a period of hours. CAUTION. While we have experienced no difficulty in handling (I), metal-organic perchlorates are potentially explosive and should be handled with due care in small quantities.

2.2. Single-crystal X-ray diffraction

Diffraction data between 100 and 300 K were collected with a Nonius KappaCCD area-detector diffractometer, using graphite-monochromated Mo $K\alpha$ radiation (λ = 0.71073 Å) from a sealed tube source. This diffractometer is fitted with an Oxford Cryostream nitrogen low-temperature device. The same crystal was used for all these data collections (0.26 × 0.23 × 0.16 mm^3), which were collected in ascending order of temperature. Intensity data were collected using ω and ϕ step scans with a scan width per frame of 1°. The detector was positioned 30 mm from the sample. The completeness of the resultant datasets lay between 97.2% at θ = 27.5° (*T* = 200 K), and 99.6% at θ = 27.5 ° (*T* = 150 K).

At 30 K, a Bruker X8 Apex diffractometer was employed with graphite-monochromated Mo $K\alpha$ radiation generated by a rotating anode (power 3 kW), and an Oxford Helix helium cryostat. A different crystal was used for this experiment (0.24 × 0.22 × 0.20 mm^3), since the original crystal had decomposed through solvent loss in the intervening time. Intensity data were collected using rotation images with a scan width of 0.5° per frame, and the detector was positioned 50 mm from the sample. The dataset was 92.7% complete to θ = 27.6°.

2.3. Data reduction

X-ray data collected at 30 K were integrated using the programs *SAINT* (Bruker, 2007), while integration of the other data used *DENZO-SMN* (Otwinowski & Minor, 1997).

Table 1
Main crystallographic features, X-ray diffraction data collection parameters and final results for (I)·2$(CH_3)_2CO$ ($C_{14}H_{14}CuN_6O_4$·$[ClO_4]_2$·$[C_3H_6O]_2$).

For all structures: $C_{14}H_{14}CuN_6O_4$·2$[ClO_4]$·2$[C_3H_6O]$, M_r = 708.91, triclinic, $P\bar{1}$, Z = 2. Experiments were carried out with Mo $K\alpha$ radiation.

	T = 30 K	T = 100 K	T = 150 K
Crystal data			
a, b, c (Å)	6.8472 (2), 13.0645 (5), 17.5942 (6)	6.8625 (2), 13.0680 (3), 17.5693 (5)	6.8970 (2), 13.1061 (3), 17.5747 (5)
α, β, γ (°)	107.211 (2), 93.712 (2), 105.976 (2)	107.2708 (17), 94.0866 (13), 105.7498 (12)	107.2954 (16), 94.5678 (12), 105.3383 (11)
V (Å^3)	1426.92 (8)	1428.16 (7)	1441.00 (7)
μ (mm^{-1})	1.02	1.03	1.03
μ (mm^{-1})	1.03	1.03	1.02
Crystal size (mm)	0.24 × 0.22 × 0.20	0.26 × 0.23 × 0.16	0.26 × 0.23 × 0.16
Data collection			
Diffractometer	Bruker X8 Apex	Nonius KappaCCD	Nonius KappaCCD
Data collection method	ω and φ scans	ω and φ scans	ω and φ scans
Absorption correction	Multi-scan†	Multi-scan†	Multi-scan†
T_{min}, T_{max}	0.822, 1.154	0.776, 0.853	0.777, 0.854
No. of measured, independent and observed [$I > 2\sigma(I)$] reflections	11 317, 6087, 5373	25 612, 6476, 5285	28 604, 6556, 5328
R_{int}	0.024	0.077	0.093
θ_{max} (°)	27.6	27.5	27.5
Refinement			
$R[F^2 > 2\sigma(F^2)]$, $wR(F^2)$, S	0.028, 0.073, 1.04	0.039, 0.108, 1.04	0.039, 0.107, 1.02
No. of reflections	6089	6476	6556
No. of parameters	406	407	407
No. of restraints	4	4	4
H-atom treatment	Mixture‡	Mixture‡	Mixture‡
$\Delta\rho_{max}$, $\Delta\rho_{min}$ (e Å^{-3})	0.47, −0.63	0.45, −0.73	0.37, −0.64

	T = 200 K	T = 250 K	T = 300 K
Crystal data			
a, b, c (Å)	7.0855 (3), 13.1506 (5), 17.2510 (8)	7.1247 (2), 13.1767 (4), 17.2946 (6)	7.1699 (2), 13.2151 (3), 17.3664 (5)
α, β, γ (°)	107.936 (3), 95.762 (2), 103.4315 (15)	107.7323 (17), 96.0184 (16), 103.5657 (13)	107.6727 (15), 96.0833 (14), 103.7596 (12)
V (Å^3)	1461.57 (11)	1475.84 (8)	1494.34 (7)
μ (mm^{-1})	1.01	1.00	0.98
Crystal size (mm)	0.26 × 0.23 × 0.16	0.26 × 0.23 × 0.16	0.26 × 0.23 × 0.16
Data collection			
Diffractometer	Nonius KappaCCD	Nonius KappaCCD	Nonius KappaCCD
Data collection method	ω and φ scans	ω and φ scans	ω and φ scans
Absorption correction	Multi-scan†	Multi-scan†	Multi-scan†
T_{min}, T_{max}	0.780, 0.856	0.782, 0.857	0.784, 0.858
No. of measured, independent and observed [$I > 2\sigma(I)$] reflections	24 551, 6483, 4699	27 221, 6636, 5229	24 994, 6655, 5396
R_{int}	0.096	0.098	0.128
Refinement			
$R[F^2 > 2\sigma(F^2)]$, $wR(F^2)$, S	0.057, 0.170, 1.03	0.058, 0.174, 1.03	0.068, 0.199, 1.03
No. of reflections	6483	6635	6655
No. of parameters	413	458	448
H-atom treatment	Constrained to parent site	Constrained to parent site	Constrained to parent site
$\Delta\rho_{max}$, $\Delta\rho_{min}$ (e Å^{-3})	0.81, −0.62	0.55, −0.67	0.64, −0.82

Computer programs used: *COLLECT* (Nonius, 1999), *APEX* 2 (Bruker–Nonius, 2004), *DENZO-SMN* (Otwinowski & Minor, 1997), *SAINT* (Bruker, 2007), *SHELXS*97, *SHELXL*97 (Sheldrick, 2008), *X-SEED* (Barbour, 2001), local program. † Based on symmetry-related measurements. ‡ Mixture of independent and constrained refinement.

The data were corrected for absorption by a multi-scan correction based on symmetry-related measurements, with the programs *SADABS* (Bruker, 2001) for the 30 K data, or *SORTAV* (Blessing, 1995) at the other temperatures. Details on data reduction are given in Table 1.[1]

[1] Supplementary data for this paper are available from the IUCr electronic archives (Reference: ZB5011). Services for accessing these data are described at the back of the journal.

2.4. Crystal structure refinements

All the structures were solved in the $P\bar{1}$ space group by direct methods (*SHELXS*97; Sheldrick, 2008), and refined by full-matrix least-squares on F^2 against all data (*SHELXL*97, Sheldrick, 2008). Calculations were carried out, and crystallographic figures were prepared, using the *XSeed* software suite (Barbour, 2001), which includes *POVRAY* (Persistence of Vision Raytracer Pty. Ltd, 2002). Atomic scattering factors

Table 2
Selected bond lengths (Å) and angles (°) for (I)·2$(CH_3)_2CO$ at 30 and 300 K.

The variation in bond lengths at other temperatures is shown in Fig. 3. The numbers in square brackets are ΔMSDA values $\langle d^2 \rangle$ (10^4 Å^2)

	300 K	30 K
Cu1—N2	1.926 (3) [15 (15)]	1.9386 (14) [21 (6)]
Cu1—N9	2.213 (3) [53 (18)]	2.1559 (14) [27 (7)]
Cu1—N12	2.210 (3) [43 (16)]	2.1567 (14) [28 (6)]
Cu1—N14	1.954 (3) [5 (14)]	1.9780 (14) [34 (6)]
Cu1—N21	2.294 (3) [18 (16)]	2.3450 (14) [19 (6)]
Cu1—N24	2.288 (3) [28 (16)]	2.3403 (14) [7 (6)]
N2—Cu1—N9	77.32 (12)	77.94 (6)
N2—Cu1—N12	77.21 (12)	77.77 (6)
N2—Cu1—N14	179.04 (11)	178.71 (6)
N2—Cu1—N21	103.98 (11)	104.84 (5)
N2—Cu1—N24	104.07 (11)	104.00 (5)
N9—Cu1—N12	154.52 (12)	155.65 (6)
N9—Cu1—N14	101.75 (12)	100.80 (5)
N9—Cu1—N21	91.86 (12)	89.06 (5)
N9—Cu1—N24	93.86 (11)	95.84 (5)
N12—Cu1—N14	103.72 (11)	103.49 (6)
N12—Cu1—N21	93.78 (11)	95.50 (5)
N12—Cu1—N24	92.75 (11)	91.63 (5)
N14—Cu1—N21	75.75 (11)	75.38 (5)
N14—Cu1—N24	76.19 (11)	75.77 (5)
N21—Cu1—N24	151.95 (10)	151.15 (5)

were taken from *International Tables for Crystallography* (1992, Vol. C, Tables 4.2.6.8 and 6.1.1.4). The TLS analyses (Dunitz *et al.*, 1988, and references therein) were performed using *THMA*11 (Trueblood, 1990), which is part of the *PLATON* suite of programs (Spek, 2003). The full experimental details and refinements results for the structure at the six temperatures are summarized in Table 1.

No disorder was present in the structures obtained at $30 \leq T \leq 150$ K. At these temperatures, all non-H atoms were refined anisotropically and all C-bound H atoms were placed in calculated positions and refined using a riding model. All O—H H atoms were located in the difference map, then allowed to refine with a common U_{iso} displacement parameter, subject to a refined O—H distance restraint. This restraint refined to a value between 0.78 (2) and 0.80 (2) Å at the different temperatures, while the refined common U_{iso} value was 0.026 (3) Å^2 at 30 K, 0.047 (4) Å^2 at 100 K and 0.057 (5) Å^2 at 150 K.

Disorder was present in the Cl and O atoms of the perchlorate anions in the three higher-temperature structure determinations. At 200 K, the Cl26–O30 anion was crystallographically ordered but the Cl31–O35 anion was disordered, and was modelled over three orientations labelled '*A*' (occupancy 0.30), '*B*' (0.30) and '*C*' (0.40). At 250 K Cl26–O30 was now disordered over two sites (labelled '*A*' and '*B*') that refined as equally occupied, while the disorder sites *A*, *B* and *C* for Cl26–O30 now had a slightly different occupancy ratio of 0.20:0.40:0.40. At 300 K, three disorder sites were refined for Cl26–O30, with occupancies of 0.40 (sites *A* and *B*) and 0.20 (site *C*). The Cl31–O35 anion was modelled over four orientations at this temperature, with occupancy 0.40 (site *A*), 0.30 (site *B*) and 0.15 (sites *C* and *D*). At these three temperatures, all disordered Cl—O bonds were restrained to a refined value of 1.43 (2)–1.44 (2) Å, and non-bonded O···O distances within a given disorder orientation were restrained to 2.34 (2)–2.35 (2) Å. The occupancies of the individual sites of anions disordered over three or four orientations were adjusted individually, until the displacement parameters in each disorder site of a particular anion were equivalent. All non-H atoms with occupancy ≥ 0.5 in the models were refined anisotropically, while all H atoms were placed in calculated positions and refined using a riding model.

2.5. Other measurements

The variable-temperature unit-cell study was performed using the aforementioned Bruker X8 diffractometer, but with an Oxford Cryostream nitrogen cryostat fitted. Variable-temperature magnetic susceptibility measurements were obtained using a Quantum Design SQUID magnetometer operating at 1000 G. A diamagnetic correction for the sample was estimated from Pascal's constants (O'Connor, 1982). A diamagnetic correction for the sample holder, and a temperature-independent paramagnetism of 60×10^{-6} cm^3 mol^{-1}, were also applied to the data.

3. Results and discussion

Six structure determinations of (I)·2$(CH_3)_2CO$ were performed, at temperatures between 30 and 300 K. The five experiments between 100 and 300 K were all run using the same crystal, but a different crystal was used for the 30 K structure. The compound adopts the $P\bar{1}$ space group at all these temperatures, and shows no gross changes in its unit cell

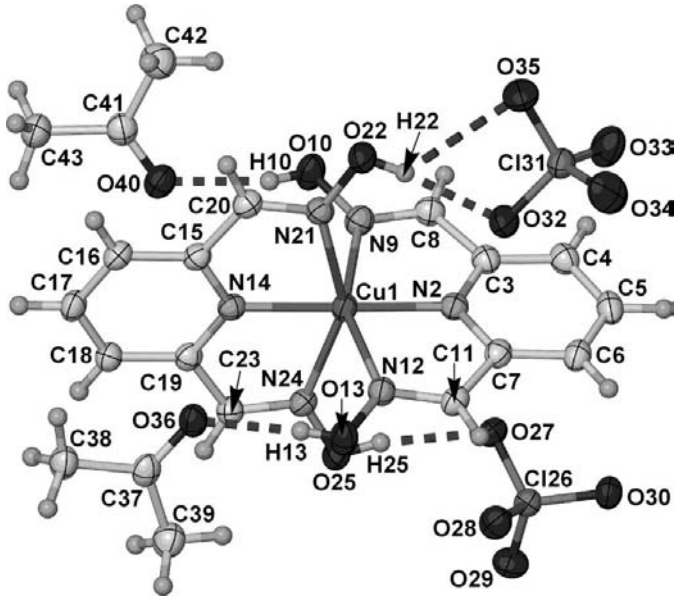

Figure 2
View of the asymmetric unit of (I)·2$(CH_3)_2CO$ at 100 K, showing the atom-numbering scheme employed. Displacement ellipsoids are at the 50% probability level except for the H atoms, which have arbitrary radii. Atom labels for C-bound H atoms, which do not take part in hydrogen bonding, are not given.

upon cooling. At room temperature the complex cation adopts a typical rhombic six-coordinate geometry with two short, two medium and two long Cu—N bonds (Fig. 2, Table 2). These bond distances, particularly for the intermediate bonds Cu1—N9 and Cu1—N12, are characteristic of a compound of this type with a $\{d_{z^2}\}^1$ configuration (structure *B*, Fig. 1; Holland *et al.*, 2000; Solanki *et al.*, 1998, 2001). The hydroxyl groups of ligand N2—O13 each donate a hydrogen bond to a different acetone molecule, while those of the other ligand N14–O25 form hydrogen bonds to the two perchlorate ions (Fig. 2), which are both strongly disordered at 300 K. The metric parameters about Cu1 are identical within 4 s.u.s at 300, 250 and 200 K (Fig. 3), and the only significant difference between these three structures is a gradual ordering of one of the perchlorate ions, Cl25–O30, which adopts a simpler disorder model at 250 K and is fully ordered in the 200 K structure.

In contrast, between 200 and 150 K two abrupt structural changes takes place. First is a shortening of the bonds Cu1—N9 and Cu1—N12 by 0.040 (3) and 0.035 (3) Å, respectively, with a concomitant increase in Cu1—N21 by 0.031 (3) and Cu1—N24 by 0.028 (3) Å (Fig. 3). The two short bonds in the complex are conformationally restrained by the surrounding ligand framework, but Cu1—N14 still shows a smaller lengthening of 0.016 (3) Å; the change in Cu1—N2 is not statistically significant. The second change is an abrupt crystallographic ordering of the other anion Cl31–O35, which is still highly disordered at 200 K but fully ordered at 150 K. Further cooling from 150 to 30 K leads to a small additional increase in Cu1—N21 and Cu1—N24, which are 0.012 (2)–0.013 (2) Å longer at 30 K compared with 150 K. The other Cu—N bonds in the molecule are equal at these two temperatures within 4 s.u.s. A comparison of the coordination geometry of the compound at 300 and 30 K is presented in Table 2 and Fig. 4. Between those temperatures, Cu1—N9 and Cu1—N12 have shortened by 0.053 (3)–0.057 (3) Å, and Cu1—N21 and Cu1—N24 have lengthened by a similar amount.

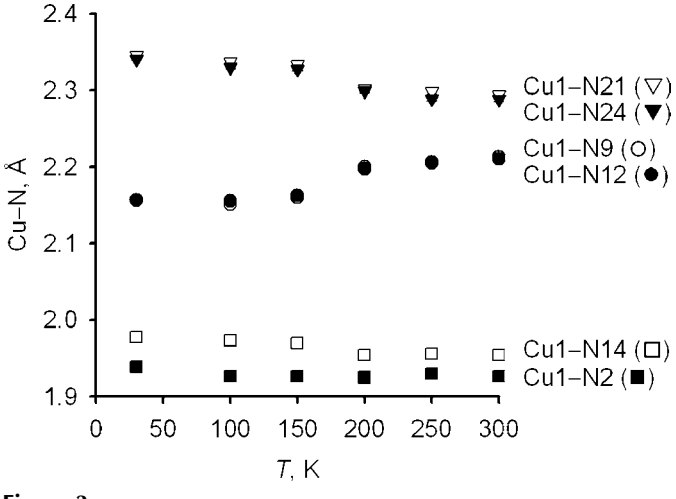

Figure 3
Temperature dependence of the Cu—N distances in (I)·2$(CH_3)_2CO$. Uncertainties are shown, but are mostly smaller than the symbols on the graph.

One possible explanation for these observations would be if the structural changes below 150 K reflected a partial, or complete, quenching of dynamic disorder of an axis of pseudo-Jahn–Teller elongation between the N9—Cu1—N12 and N21—Cu1—N24 directions in (I). Such quenching of Jahn–Teller disorder is well known in copper(II) compounds (see *e.g.* Halcrow, 2003, and references therein; Kilner *et al.*, 2004; Simmons *et al.*, 2005; Beddard *et al.*, 2003). This can be tested through a TLS analysis to determine the mean-square displacement amplitudes (MSDAs) for the Cu—N bonds in the molecule (Dunitz *et al.*, 1988). The difference between the MSDAs for the two atoms in each bond ($\langle d^2 \rangle$, Table 2) is a fingerprint for the presence of hidden disorder in that bond; if the molecule possesses hidden Jahn–Teller disorder, then $\langle d^2 \rangle$ for the bonds involved in that disorder should be high. In practise, for copper(II) complexes of N-donor ligands, a $\langle d^2 \rangle$ value $> 100 \times 10^{-4}$ Å^2 for any Cu—N bond in the molecule indicates that Jahn–Teller disorder might be present (Falvello, 1997, and references therein). If that disorder is dynamic, then those values should be temperature-dependent.

The $\langle d^2 \rangle$ values for the Cu–N bonds in (I)·2$(CH_3)_2CO$ at 30 and 300 K are listed in Table 2. Although the errors are large, as normal, $\langle d^2 \rangle$ for each bond is identical within 3 s.u.s at the two temperatures and is also within 3 s.u.s of zero. Data from the intermediate temperatures are similar, with the maximum value of $\langle d^2 \rangle$ at any temperature being 53 (18) $\times 10^{-4}$ Å^2 (for the bond Cu1—N9 at 300 K, Table 2). Hence, there is no evidence for hidden Jahn–Teller disorder in (I)·2$(CH_3)_2CO$, and the observed structural changes reflect a genuine change in the conformation of the complex.

Comparison of the high- and low-temperature structures shows that a substantial rearrangement within the asymmetric

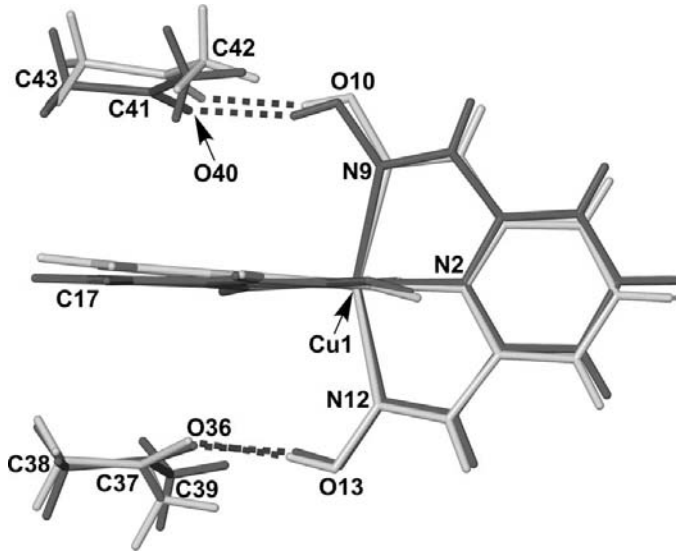

Figure 4
Overlay of the $[Cu(L^{OH})_2]^{2+}$·2$(CH_3)_2CO$ moiety in (I)·2$(CH_3)_2CO$ at 300 K (pale) and 30 K (dark), highlighting the changes in the conformation of the cation and the positioning of the solvent on cooling. For clarity the perchlorate ions are not shown, since these are badly disordered in the high-temperature structure. See Fig. 2 for the full atom-numbering scheme.

unit has taken place, with several non-H atoms having shifted by up to 0.5 Å between the two temperatures (Fig. 4). Apart from the crystallographic ordering of the anions, the largest changes are associated with acetone solvent molecules and the residues in the cation that interact directly with them. The C and O atoms in solvent molecule O40–C43 at 30 K are displaced by 0.32–0.50 Å from their corresponding positions at 300 K. This is accompanied by a similar movement of O10, which hydrogen bonds to this solvent molecule, by 0.32 Å between the two temperatures. The pyridine ring N14–C19 is in van der Waals contact with the same solvent molecule, and also moves in concert with it on cooling. The dihedral angle of the least-squares plane of this ligand with the equatorial plane of the complex (formed by N2, N14, N21 and N24) decreases from 1.75 (9)° at 300 K to 0.87 (4)° at 30 K, resulting in a lateral displacement of 0.24–0.30 Å for C16–C18. The position of the C39 methyl group also shifts by 0.50 Å between 300 and 30 K, but the movements of the other atoms in that solvent molecule, O36–C38, are $\leq$ 0.16 Å. Hence, the position of O13 (which hydrogen bonds to O36) does not change significantly between the two temperatures. The positions of the other atoms in the complex, which interact directly with the anions by hydrogen bonding or van der Waals contacts, show smaller changes on cooling of $\leq$ 0.25 Å (Fig. 4).

A variable-temperature unit-cell study of (I)·2$(CH_3)_2$CO showed a discontinuity on cooling from 160 to 155 K, most strongly in a 0.34 (3) Å increase in c and a 1.7 (2)° increase in γ (Fig. 5). The other unit-cell angles also show smaller changes at the same temperature (Fig. 5). These changes are not reflected in V, however, which decreases monotonically within experimental error between 300 and 100 K before levelling out below that temperature. Hence, the anion ordering and structural rearrangement observed between 150 and 200 K occur abruptly, at 157 $\pm$ 3 K.

The structural rearrangement of the ligand sphere in (I)·2$(CH_3)_2$CO around 157 K should be reflected in a change in the g values of the copper(II) ion (Goodman & Raynor, 1970). Unfortunately, the EPR spectra of powdered, solvent-free (I) are inconclusive. Consistent with the structural changes in the single crystal they are temperature dependent, but the low-temperature spectra are contaminated by intermolecular dipolar interactions that prevent their accurate simulation (Halcrow *et al.*, 2004). However, such a change should also be reflected in the magnetic moment of the compound, which is proportional to $\langle g \rangle^2$ (O'Connor, 1982). At room temperature, (I) shows $\chi_M T = 0.42$ cm^3 mol^{-1} K, in good agreement with the value expected from its room-temperature EPR spectrum ($\langle g \rangle$ = 2.132; Halcrow *et al.*, 2004). This value decreases slightly upon cooling, reaching a value of 0.40 cm^3 mol^{-1} K at 5 K (Fig. 6). Importantly, the curve shows a discontinuity between 130 and 150 K that, although small, is above the noise level of the data. This can be attributed to the changes in the Cu—N bond length taking place following

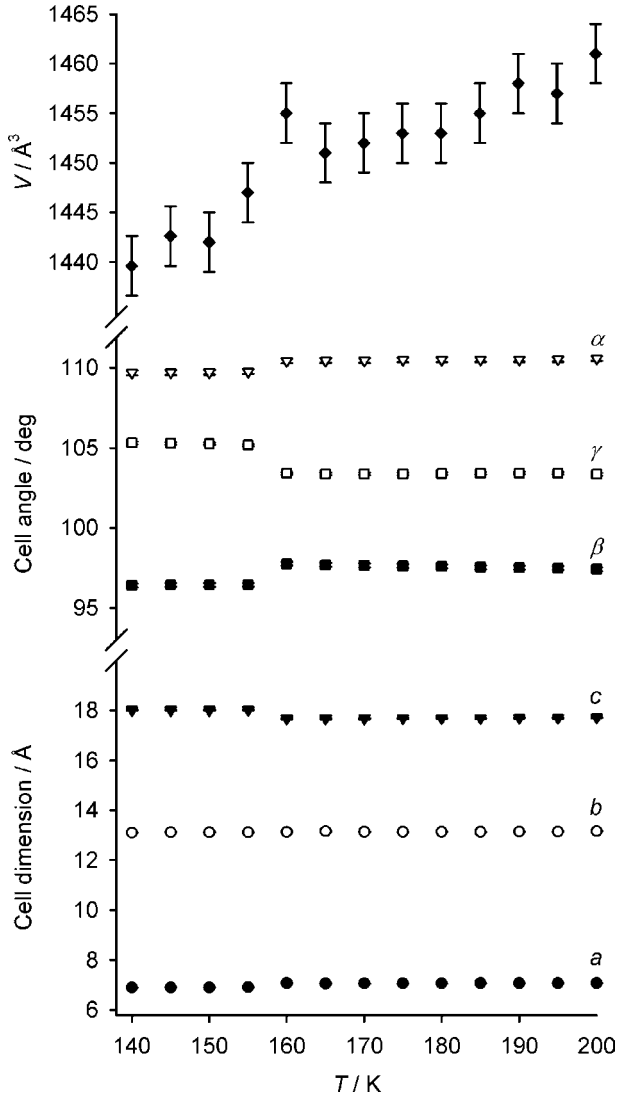

Figure 5
Variation of the unit-cell parameters in (I)·2$(CH_3)_2$CO with temperature. Uncertainties are shown, but are often smaller than the symbols on the graph.

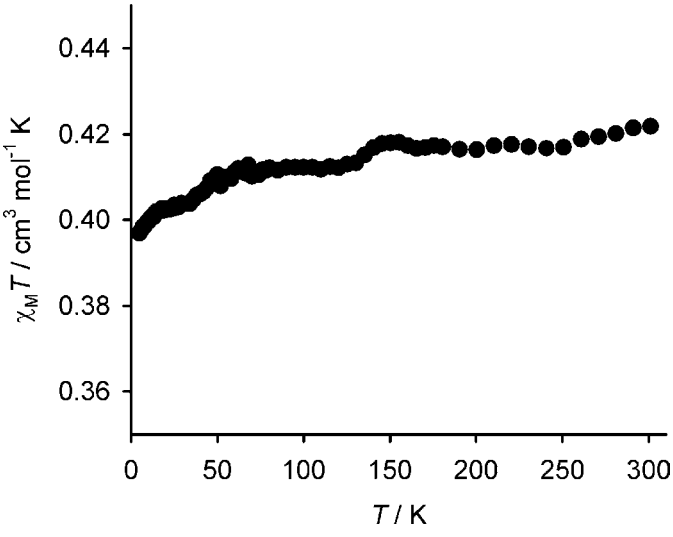

Figure 6
Variable-temperature magnetic susceptibility data for (I). The discontinuity between 130 and 150 K can be attributed to the structural rearrangement associated with perchlorate anion ordering observed in the single-crystal study.

anion ordering, as seen in the single crystal. The apparently slightly lower temperature of the transition in powdered (I), compared with (I)·2$(CH_3)_2CO$, might reflect small changes in anion mobility following the loss of solvent in the dried material. The small additional decrease in $\chi_M T$ below 50 K is commonly observed in solid molecular paramagnets, and probably reflects the influence of weak intermolecular superexchange or dipolar interactions in the material (O'Connor, 1982).

4. Conclusion

Our initial study of (I), and of the corresponding hydrazone complex (II), concluded that both compounds show a temperature-dependent electronic structure (Halcrow *et al.*, 2004). This was suggested by the crystal structure of (I)·2$(CH_3)_2CO$, which showed significant differences at 300 and 100 K; and a variable-temperature EPR study of (II), which has the form expected of a $\{d_{z^2}\}^1$ species at room temperature but evolves to a $\{d_{x^2-y^2}\}^1$ lineshape at 5 K. This more detailed study of (I)·2$(CH_3)_2CO$ has clarified the origin of these effects. An abrupt order/disorder transition of one of the two perchlorate anions in the asymmetric unit at 157 (3) K is accompanied by a rearrangement of the coordination sphere about the copper ion, from structure *B* towards structure *A* as the crystal is cooled (Fig. 1), and by a significant displacement of the acetone solvent molecules. The change in Cu—N bond lengths accompanying the transition is reflected in a small reduction in the magnetic moment of the dried material about the transition temperature.

It is uncertain whether the structural relaxation of the copper centre, or the anion-ordering event, is responsible for triggering the structural rearrangement near 157 K. However, it is clear that the electronic structure of the $[Cu(L^{OH})_2]^{2+}$ cation is unusually plastic, and can be modified by a change in its local environment. An appropriately substituted $[Cu(L^R)_2]^{2+}$ centre that is similarly sensitive might be used as a reporter group for sensor applications, by changing its Jahn–Teller structure in response to guest-binding or another physical stimulus.

The authors thank Dr Harry Blythe (University of Sheffield) for the magnetic susceptibility data, while MAH thanks the Research Centre for Materials Science, Nagoya University, for a sabbatical that allowed the writing of this paper. This work was funded by the EPSRC and the University of Leeds.

References

Barbour, L. J. (2001). *J. Supramol. Chem.* **1**, 189–191.
Beddard, G. S., Halcrow, M. A., Hitchman, M. A., de Miranda, M. P., Simmons, C. J. & Stratemeier, H. (2003). *Dalton Trans.* pp. 1028–1032.
Blessing, R. H. (1995). *Acta Cryst.* A**51**, 33–38.
Bridgeman, A. J., Halcrow, M. A., Jones, M., Krausz, E. & Solanki, N. K. (1999). *Chem. Phys. Lett.* **314**, 176–181.
Bruker (2001). *SADABS*. Bruker AXS Inc., Madison, Wisconsin, USA.
Bruker (2007). *SAINT*. Bruker AXS Inc., Madison, Wisconsin, USA.
Bruker–Nonius (2004). *APEX*2. Siemens Analytical X-ray Instruments Inc., Madison, Wisconsin, USA.
Dunitz, J. D., Schomaker, V. & Trueblood, K. N. (1988). *J. Phys. Chem.* **92**, 856–867.
Falvello, L. R. (1997). *J. Chem. Soc. Dalton Trans.* pp. 4463–4475.
Goodman, B. A. & Raynor, J. B. (1970). *Adv. Inorg. Chem. Radiochem.* **13**, 135–362.
Halcrow, M. A. (2003). *Dalton Trans.* pp. 4375–4384.
Halcrow, M. A., Kilner, C. A., Wolowska, J., McInnes, E. J. L. & Bridgeman, A. J. (2004). *New J. Chem.* **28**, 228–233.
Hitchman, M. A. (1994). *Comments Inorg. Chem.* **15**, 197–254.
Holland, J. M., Liu, X., Zhao, J. P., Mabbs, F. E., Kilner, C. A., Thornton-Pett, M. & Halcrow, M. A. (2000). *J. Chem. Soc. Dalton Trans.* pp. 3316–3324.
Kilner, C. A., McInnes, E. J. L., Leech, M. A., Beddard, G. S., Howard, J. A. K., Mabbs, F. E., Collison, D., Bridgeman, A. J. & Halcrow, M. A. (2004). *Dalton Trans.* pp. 236–243.
Mazej, Z., Arčon, I., Benkič, P., Kodre, A. & Tressaud, A. (2004). *Chem. Eur. J.* **10**, 5052–5058.
Murphy, B. & Hathaway, B. (2003). *Coord. Chem. Rev.* **243**, 237–262.
Nonius (1998). *COLLECT*. Nonius BV, Delft, The Netherlands.
Obert, T. & Bersuker, I. B. (1983). *Czech. J. Phys. B*, **33**, 568–573.
O'Connor, C. J. (1982). *Prog. Inorg. Chem.* **29**, 203–283.
Ooijen, J. A. C. van, van der Put, P. J. & Reedijk, J. (1977). *Chem. Phys. Lett.* **51**, 380–382.
Otwinowski, Z. & Minor, W. (1997). *Methods in Enzymology*, Vol. 276, *Macromolecular Crystallography*, Part A, edited by C. W. Carter & R. M. Sweet, pp. 307–326. New York: Academic Press.
Persistence of Vision Raytracer Pty. Ltd (2002). *POVRAY*, Version 3.5. Persistence of Vision Raytracer Pty. Ltd, Williamstown, Victoria, Australia; http://www.povray.org.
Riley, M. J., Hitchman, M. A., Reinen, D. & Steffens, G. (1988). *Inorg. Chem.* **27**, 1924–1934.
Salaudeen, A. A., Kilner, C. A. & Halcrow, M. A. (2008). *Chem. Commun.* pp. 5200–5202.
Sheldrick, G. M. (2008). *Acta Cryst.* A**64**, 112–122.
Simmons, C. J., Stratemeier, H., Hanson, G. R. & Hitchman, M. A. (2005). *Inorg. Chem.* **44**, 2753–2760.
Solanki, N. K., Leech, M. A., McInnes, E. J. L., Zhao, J. P., Mabbs, F. E., Feeder, N., Howard, J. A. K., Davies, J. E., Rawson, J. M. & Halcrow, M. A. (2001). *J. Chem. Soc. Dalton Trans.* pp. 2083–2088.
Solanki, N. K., McInnes, E. J. L., Mabbs, F. E., Radojevic, S., McPartlin, M., Feeder, N., Davies, J. E. & Halcrow, M. A. (1998). *Angew. Chem. Int. Ed.* **37**, 2221–2223.
Spek, A. L. (2003). *J. Appl. Cryst.* **36**, 7–13.
Trueblood, K. N. (1990). *THMA*11. University of California, Los Angeles, USA.